Analysis of Weld Induced Distortion of Butt Joint using Simulation and Experimental Study

Mohd Shahar bin Sulaiman*
Yupiter HP Manurung
Faculty of Mechanical Engineering, UiTM Shah Alam

Marcel Graf
Alexander Bauer
Professorship of Virtual Production Engineering,
Chemnitz University of Technology, Germany

*msbsn2212@yahoo.com

ABSTRACT

This paper focuses on investigation of welding distortion that occurred due to GMAW process which can adversely affect the dimensional accuracy and aesthetical value of the welded structure. Distortion can lead to production delay and costly remedial work. Based on this fact, it is necessary to predict the welding distortion in advance in order to produce high quality welded parts and thus to reduce production cost. In this study, the welding distortion induced in butt joint with thickness of 4 mm was simulated using Finite Element Method (FEM) software Simufact.Welding Version 5. The welding deformation was computed based on non-linear thermo-elastic-plastic numerical analysis. Low carbon steel material was employed for the simulation and experimental study. A series of experiments using fully automated welding process were carried out for verification purpose in order to measure the distortion. By comparing the results between simulation and experiment, it was found out that a good agreement was achieved and fast solution analysis time was provided in predicting weld induced distortion.

Keywords: *FEM, GMAW, Numerical analysis, Simufact, Welding distortion.*

Introduction

A joining process that produces coalescence of metals with or without the application of filler metal or pressure by heating them to the welding temperature is known as welding [1,2]. Welding can be considered as the most economical, versatile and efficient method to permanently join metallic materials. Products joined by welding will always become less expensive compared to products that made by other manufacturing processes if it is designed intelligently. Therefore, welding has been extensively applied in many industries as the principal method of fabricating and assembling numerous metallic products such as in shipbuilding, building construction, aircraft manufacturing and automotive industries [3,4,5].

In addition, GMAW is also known as a very flexible process which could be utilized for joining all metals [6]. In response to high complexity, productivity and quality as well as an enormous variety of products, highly automated welding process using robot has been introduced especially involving advanced GMAW process [7].

Distortion is an undesirable dimensional change of a fabrication that is produced by high temperature heat employed in the welding process [8]. Temperature variations triggered by the transient heat source in welds and parent metals during the welding process lead to non-uniform temperature distributions across the weldment and in the parent metals and thus can result in residual stresses induced distortions [9].

Nowadays, the increasingly growth in computer performance and rapid developments in numerical methods have allowed faster and more accurate predictions of computer modelling [10]. The application of welding simulation has significantly become important especially to avoid or minimize post processing work, thus could enhance the welded parts' quality and also enable to reduce the production cost. There are a lot of different welding simulation methods [11,12,13] such as 3D applied plastic strain method, 3D thermal elastic-plastic finite element analysis and local stress-life/fracture mechanics approach that can be utilized in order to predict welding deformations, residual stresses as well as fatigue life respectively.

In this study, non-linear thermo-elastic-plastic analysis method using FEM software Simufact.Welding was employed to simulate the welding process and to predict the welding distortion in butt joint with the thickness of 4 mm. For verification purpose, a series of experiments were also performed using fully automated welding system with GMAW power source. The shielding gas used for the welding process was a mixed gas consisting of argon (Ar) and carbon dioxide (CO_2). To measure the initial and final dimensions of the specimen, a coordinate measuring machine (CMM) was applied.

Experimental Set-Up and Procedure

For verification purpose, a series of experiments were carried out using robotic welding ABB IRB 2400/16 with GMAW power source KEMMPI ProEvolution ProMIG 540 MXE as displayed in Figure 1. Nowadays, robotic welding is recognized as a mature production method which has a flexible movement pattern using six axes. The advantage of a robotic welding system is that one single point remote robot control unit can be used to perform all welding parameters and robot programming [14].

Figure 1: Welding robot and apparatus used in experiment

The edges of the 4 mm low carbon steel specimens for the butt joint were prepared by grooving a 60°-included angle. Prior to the experiments, both plates were tacked using GTAW. Figure 2 shows the clamping condition assigned during the welding process. Filler wire with AWS Classification of ER70S-6 and 1.2 mm in diameter was used throughout this study.

Figure 2: Clamping conditions applied for butt joint

Table 1: Welding parameters used for experimental investigation

Parameters	Butt Joint
	Values
Current, I (A)	140 - 160
Voltage, V (V)	17 - 20
Travel speed, v (mm/s)	4
Wire feed speed, u (m/min)	3.5 – 4.0
Shielding gases, Ar / CO_2 (%)	80 / 20

The welding parameters that had been used during the experiments were tabulated in Table 1. Prior to the welding process, the specimens of butt joint were measured to gain the initial readings of specific points on the specimens. The measurement was conducted using Coordinate Measuring Machine (CMM) model Mitutoyo 707 as illustrated in Figure 3. After the welding process and sufficient time for cooling to room temperature, the specimens were once again measured using the same machine to obtain the final readings of the identical points that had been measured before. The measuring points (3 points) involved were marked as shown in Figure 4. Then, the actual angular distortion (average) could be defined by measuring the relative values between before and after the welding process.
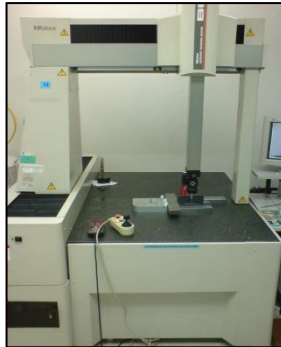

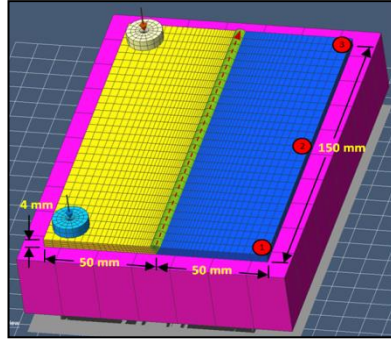Figure 3: Coordinate Measuring Machine used for measurement of distortion

Figure 4: Butt joint model utilized for simulation

Welding Simulation Method and Procedure

Geometrical Modelling

A schematic illustration of solid FE model of butt joint used in the simulation is displayed in Figure 4. The model comprises two symmetrical plates with a plate of size 50 mm x 150 mm x 4 mm. A weld bead for the joint is also modelled in which the welding trajectory is located. The clamping condition defined in the simulation (downward arrows) as shown in Figure 4 was similar to that of experiment as exhibited in Figure 2.

Material Modelling

In welding simulation, low carbon steel material (S355J2G3) had been used for estimating the distortion. The material was selected in accordance with the experiment. Table 2 presents the chemical composition of the materials utilized in the simulation and experiment, in which the experimental results were obtained using an Arc Spark Emission Spectrometer with pure argon of 99.9% and its software called Spark Analyzer MX.

Table 2: Chemical composition of materials

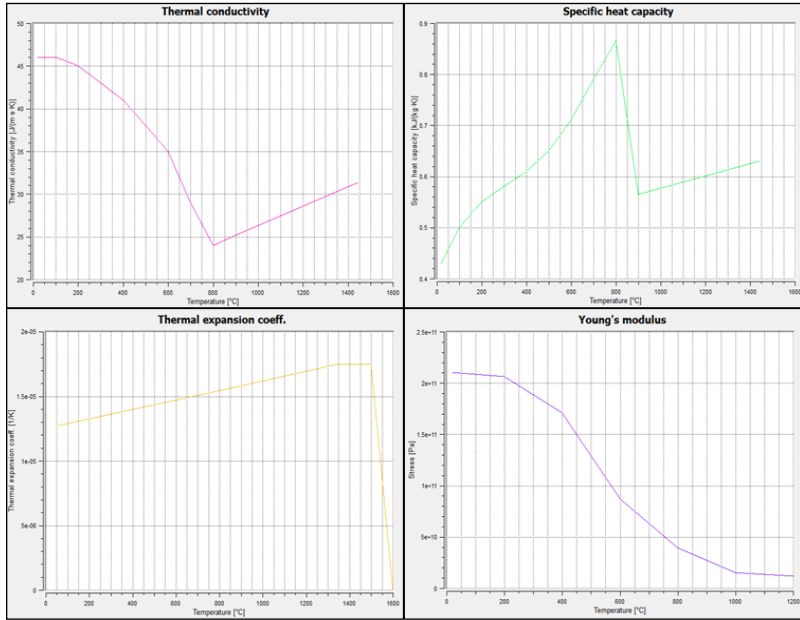| Elements	S355J2G3 (%)	Experiment (%)
C	0.170	0.186
Mn	1.600	0.146
Si	0.020	0.011
S	0.011	0.0011
P	0.017	0.001

Figure 5: Temperature-dependent material properties

In simulation, all the computations were made based on analysis using temperature-dependent material properties as shown in Figure 5. In welding process, the workpiece was heated up to its melting temperature especially in heat affected zone (HAZ) area and the weldment itself. Due to this phenomenon, the values of material properties would change according to the temperature variation. The temperature-dependent material properties were very important since it would reflect the real situation that occurred to the workpiece during the welding process. If the simulation executed using constant material properties, it will consider the material behaviour at room temperature only which in turn can lead to incorrect prediction. In addition, another mechanical property which is Poisson's ratio was assumed to be 0.3 that was not dependent on temperature.

Heat Source Modelling
In welding simulation, one of the most important steps is to model the heat source. Suitable heat source model must be selected in accordance with the welding process. Hence, for GMAW process, double ellipsoid model was employed to replicate the real heat source. The double ellipsoid model was defined by Goldak [10]. The subsequent Equation (1) was used to characterize the power density distribution inside the front and rear quadrants

of the heat source which were denoted by subscripts 1 and 2 correspondingly. In this equation, Q represents the power input, v stands for the travel speed, t denotes the time, τ refers to a lag factor at $t = 0$, f_1 and f_2 are the fractions of heat deposited in the front and rear quadrants respectively, whereas a, b and c define the heat source dimensions. The configuration of double ellipsoid model is illustrated in Figure 6.

$$q_{1,2}(x,y,z,t) = \frac{6\sqrt{3}f_{1,2}Q}{abc_{1,2}\pi\sqrt{\pi}}\,e^{-3x^2/a^2}\,e^{-3y^2/b^2}\,e^{-3[z+v(\tau-t)]^2/c_{1,2}^2} \tag{1}$$
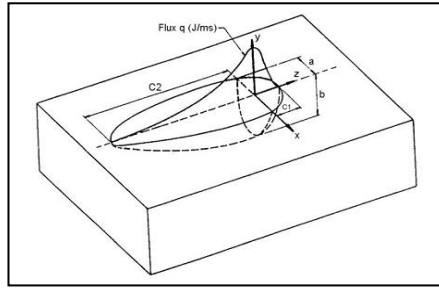

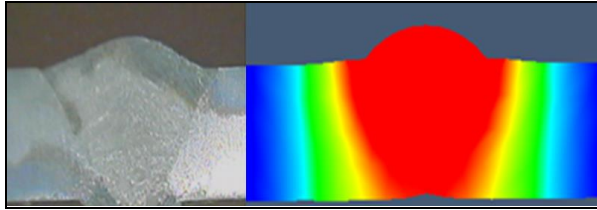Figure 6: Double ellipsoid heat source configuration

Figure 7: Macrographs of specimen (left) and predicted
weld fusion zone (right)

The heat source used in simulation was calibrated by comparing the temperature contour plot of predicted weld fusion zone with the actual macrograph obtained through experiment as exhibited in Figure 7. In this simulation, the heat source parameters of a (width), b (depth), c_1 (front length) and c_2 (rear length) involved were 2.5 mm, 5.2 mm, 2.5 mm and 5.0

mm respectively. Similar welding parameters to experiment were employed during the calibration.

Boundary Conditions

There were two types of boundary conditions involved in the welding simulation which consist of thermal and mechanical boundary conditions. The thermal boundary conditions were defined by heat losses as the results of convection and radiation as well as conduction between two bodies, while the mechanical boundary condition was defined by clamping condition. Figure 4 demonstrates the clamping models employed in the simulation study. They were modelled as rigid bodies and worked as springs to prevent body motion by applying a force opposite to a movement normal to the surface.

Simulation Method

In this simulation, all the calculations were made based on non-linear thermo-elastic-plastic analysis using the geometrical, material and heat source models which have been explained previously. Referring to Figure 4, the red arrow indicates the welding direction defined during the welding simulation. All the defined boundary conditions were taken into account especially to compute the cooling behaviour of the model that would influence the final predicted results. The total strain (ε_{total}) was computed through the combination of elastic (ε_e), plastic (ε_{pl}) and thermal (ε_{th}) strains, in which the phase transformations were also taken into consideration for the thermal strain computation as expressed by Equation (2).

$$\varepsilon_{total} = \varepsilon_e + \varepsilon_{pl} + \varepsilon_{th} \tag{2}$$

Results and Discussion

After the welding simulation was completed, the postprocessing analysis could be implemented in which the angular distortion triggered by the welding process could be observed. Figure 8 and Figure 9 display the predicted and actual results of angular distortions respectively. Table 3 presents the average value of distortion estimated via simulation and also the average value of distortion obtained by means of experimental method. The average value on the unclamped side was determined from the points as specified in Figure 4.
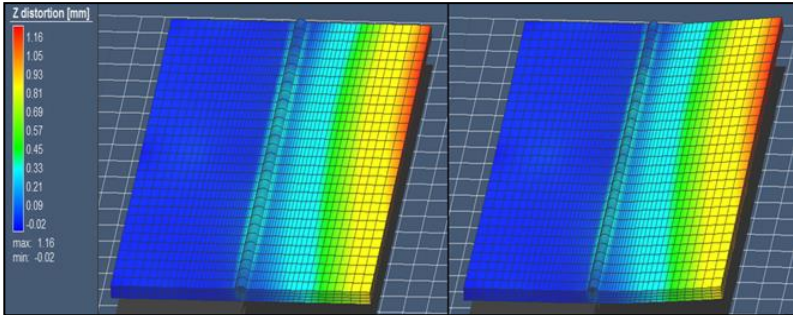
Figure 8: Angular distortion of butt joint without magnification (left) and with 3x magnification (right)

Figure 9: Angular distortion of specimen

Table 3: Comparison of angular distortion results between simulation and experimental methods

Methods	Distortions		Error Percentage
	(mm)	(rad)	(%)
Simulation	1.02	0.0204	9.73
Experiment	1.13	0.0226	

From the figures in the table, it can be seen that the predicted result was slightly different than that of experimental measurement. By looking through the deformed shape of simulated result, it was clearly confirmed that

the predicted pattern was nearly similar to that of real deformation. The magnification factor used in Figure 8 was just to show of how the workpiece deformed after the welding process in which the values of distortion remained unchanged. In addition, it could be observed that the angular distortion in the base metal of butt joint occurred in upward direction on the unclamped side. The deformation took place upward gradually starting from the welded region towards the edge of the unclamped base plate. This condition caused the maximum distortion to occur at the edge of the unclamped side. Conversely, due to the clamping effect, there was considerably negligible distortion on the clamped side of base metal and also at the welded region of the joint.

After the deposition of weld metal, the cooling cycle would lead to contraction of the weld metal. This phenomenon would generate shrinkage forces in consequence of residual stresses which induced after all the external constraints had been released. The existence of the shrinkage forces subsequently would trigger off the formation of bending moments and therefore, caused the unclamped base plate to distort.

Conclusions

From the analysis of the results, it was found that a good agreement had been achieved between finite element simulation and experimental verification. This outcome revealed that the capability and reliability of finite element analysis using non-linear thermo-elastic-plastic method performed through Simufact.Welding had been obviously proven in forecasting welding distortion sensibly. In order to obtain a good prediction, the heat source model employed must be well calibrated, and the defined boundary conditions should reflect the real welding process. Furthermore, another aspect that contributed to a good prediction was the correct material modelling. In this study, temperature-dependent material properties had been implemented which were closer to reality. However, the deviating result between simulation and experiment might be arisen from the factors such as slight differences in material properties, chemical composition, geometry as well as thickness. Regarding time and effectiveness, the executed simulation method was ideal and practical to be applied for simulating welding distortion and hence, this software possesses a great potential for identifying distortion in more complex welded joints. Therefore, the significant impact from this research proved that the welding distortion which is inevitable and difficult to predict, seems possible to be estimated and as a result the control of distortion can be wisely planned in advance prior to the commencement of the real welding process. Thus, it allows and enables us to particularly devise a good and reliable welding procedure.

Acknowledgement

References

[1] Frank M. Marlow, Welding Fabrication & Repair, 1st ed. (Industrial Press Inc., New York, 2002).

[2] John Norrish, Advanced Welding Processes, (Woodhead Publishing Limited, Cambridge, England, 2006).

[3] Mohd Shahar Sulaiman, Yupiter HP Manurung, Robert Ngendang Ak. Lidam, Mohd Ridhwan Redza, Mohammad Ridzwan Abdul Rahim, Shahfuan Hanif Ahmad Hamidi, Esa Haruman, Sunhaji Kiyai Abas and Ghalib Tham, "Analysis of weld induced distortion of double sided T-joint using simulation and experimental study," Proceedings of the 2010 International Conference on Advances in Mechanical Engineering, 78 - 82 (2010).

[4] B. J. Moniz and R. T. Miller, Welding Skills, (American Technical Publishers Inc., United States of America, 2004).

[5] V. H. Baltazar Hernandez, M. L. Kuntz, M. I. Khan and Y. Zhou, "Influence of microstructure and weld size on the mechanical behavior of dissimilar AHSS resistance spot welds," Science and Technology of Welding and Joining 13, 769 - 776 (2008).

[6] R.S. Parmar, Welding Engineering and Technology, (Khanna Publishers, New Delhi, 2010).

[7] J. Norberto Pires, Altino Loureiro and Gunnar Bolmsjö, Welding Robots, (Springer Science+Business Media Inc., Germany, 2006).

[8] Howard B. Cary, Modern Welding Technology, 3rd ed. (Prentice Hall, New Jersey, 1994).

[9] H. Long, D. Gery, A. Carlier and P.G. Maropoulos, "Prediction of welding distortion in butt joint of thin plates," Materials and Design 30, 4126 - 4135 (2009).

[10] John A. Goldak and Mehdi Akhlaghi, Computational Welding Mechanics, (Springer Science+Business Media Inc., United States of America, 2005).

[11] L. Zhang, P. Michaleris and P. Marugabandhu, "Evaluation of applied plastic strain methods for welding distortion prediction," Journal of Manufacturing Science and Engineering 129 (6), 1000 - 1010 (2006).

[12] Chin-Hyung Lee and Kyong-Ho Chang, "Prediction of residual stresses in welds of similar and dissimilar steel weldments," Journal of Materials Science 42, 6607 - 6613 (2007).

[13] P. Johan Singh, D.R.G. Achar, B. Guha and Hans Nordberg, "Fatigue life prediction of gas tungsten arc welded AISI 304L cruciform joints with different LOP sizes," International Journal of Fatigue 25, 1 - 7 (2003).

[14] K. Weman and G. Lindén, MIG Welding Guide, (Woodhead Publishing Limited, Cambridge, England, 2006).